12-1-2006

Why Do Descending Shells Around Cumulus Clouds Exist?

Thijs Heus
Delft University of Technology, t.heus@csuohio.edu

Harm J.J. Jonker
Delft University of Technology

2.8 WHY DO DESCENDING SHELLS AROUND CUMULUS CLOUDS EXIST?

Thijs Heus*and Harm J.J. Jonker,
Mult-Scale Physics, Delft University of Technology, The Netherlands

1. INTRODUCTION

In search of better descriptions of shallow cumulus clouds, the main focus lies more and more on the dynamical properties and microphysical structure of the clouds and on its interaction with the environment (e.g. (Siebesma and Cuijpers, 1995)). For this type of study, sufficient statistics of the three dimensional flow are needed, which is usually better provided by Large Eddy Simulations (LES) than by experimental data, which often can provide one- (e.g. airplane measurements) or two-dimensional (satellites) data. While LES has proven to be an extremely useful tool to investigate these cloud dynamics, comparisons between LES and experimental remains desireable. Usually, (e.g. (Siebesma et al., 2003), (Stevens et al., 2001) and (Neggers et al., 2003)) only slab-averaged fields and derived quantities are compared with observations. This study focuses on detailed lateral profiles of the main (thermo)dynamic variables, conditionally averaged over clouds and surroundings similar to the study by (Rodts et al., 2003) on observational data (From here onwards referred to as [RDJ03]). The method of post-processing used by [RDJ03] is based on a method where the 1-D data is conditionally averaged over the cloud and its environment. This resulted in lateral profiles of the various properties of the cloud as a function of the normalized horizontal position in the cloud. Not only the average values were obtained in this way, but also the variance around these averages, which can be seen as an estimate for the turbulence. Comparing [RDJ03] with LES provides a new and interesting validation of the detailed dynamical structure of the simulations. To obtain optimal comparison, the post processing of the numerical results is closely modeled to the method used for the observational data enabling direct comparison and providing insight in a natural way.

Emphasis will be placed on the role of a shell of descending air found around shallow cumulus clouds not only by [RDJ03], but also reported in earlier studies (e.g. (Jonas, 1990), abbreviate as [J90]). Discussion on this shell is usually directly linked to the significance of lateral mixing over cloud edge. In literature (e.g. (Paluch, 1979), (Blyth, 1993)), lateral mixing is considered to be of much less importance to cloud dynamics than cloud-top mixing. If this also holds for this shell, as [J90] suggested, the shell has to be driven by a mechanical forcing through the pressure-gradient force. However, this is questioned by [RDJ03], who advocates that the descending motion is driven by evaporative cooling following lateral mixing over the cloud edge, thus creating negatively buoyant air around the cloud (see figure 1). Unfortunately both studies could not be conclusive due to the lack of sufficient observational data, especially since no directcould be. Summarizing, there is some observational evidence and theoretical backup for the role of evaporative cooling as well as for mechanical forcing. This study aims to use the controllable environment of LES to study this subsiding shell using the complete three-dimensional fields of all variables, while ensemble averaging over many statistically independent simulations can ensure reliable statistics. Finally an analytical model is setup to describe the cloud/shell/environment system in a qualitative way.

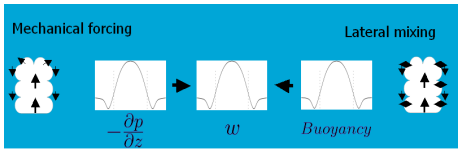

FIG. 1: Two different mechanisms are hold responsible for the shell of subsiding air around clouds; a mechanical forcing would show in the vertical pressure gradient, while lateral mixing over the cloud edge would result in a buoyancy drop, leading to the vertical velocity dip.

2. EXPERIMENTAL SETUP

A parallelized LES model is used (e.g. (Cuijpers and Duynkerke, 1993)). Since the observations of [RDJ03] were based on the Small Cumulus Microphysics Study (SCMS), an LES-case based on SCMS is used to perform the numerical simulations ((Neggers et al., 2003)). Simulations were carried out on a domain of $6.4km \times 6.4km \times 5.12km$ with each cell of a size of $\Delta x = \Delta y = 1.25\Delta z = 50m$. While the SCMS case is needed for comparison with observations, it suffers from several limitations. Most importantly, the diurnal cycle allows only a small window in time to obtain data from and prevents the atmosphere from reaching a steady state. To overcome these issues, and to investigate whether features observed in SCMS are case-specific or not, several simulations are run with a BOMEX based case ((Siebesma et al., 2003)). These simulations are carried out on a domain of $6.4km \times 6.4km \times 3.2km$ and a grid box of $\Delta x = \Delta y = 1.25\Delta z = 25m$. The runs are done for 12 hours, from which the first 3 hours are discarded as spin-up. To further improve statistics, these simulations are carried out 10 times with a different random perturbation to create statistically independent runs. To rule out the possibility that a possible thin shell is due to the numerical integration scheme, both a central differencing and a

* *Corresponding author address:* Thijs Heus, Dept. of Multi-Scale Physics, Delft University of Technology, Lorentzweg 1, 2628CJ Delft, The Netherlands, e-mail: t.heus@tudelft.nl

monotonous scheme are used. Only the results obtained with the central differencing scheme are shown here.

2.1 *Method of postprocessing*

The used method of postprocessing aims to mimic a plane doing line measurements. In analogy to [RDJ03], measurements are done back and forth through the dataset in both x- and y- direction. Following one such track, observational variables (w, θ_l, q_t and q_l) are sampled for points within a cloud or within one cloud length distance from both sides of the cloud.The average value of the region before the cloud was subtracted from all the values, and the results are averaged over all clouds. Whereas [RDJ03] needed to use all clouds larger than $500m$ in their statistics to gain reliable statistics, here we are able to select only clouds with a horizontal size of exactly $400m$. This strict size specification ensured that no rebinning needed to be done, which could average out much of the signal, especially on the discrete LES grid. The slight reduction in size to $400m$ ensured that enough clouds exist for reliable statistics.

If on a certain line of measurement one of the environmental points happens to fall inside another cloud, this entire line is discarded in the statistics. Data can be acquired over all heights or over all cloud sizes larger than or equal to a threshold size. Data within one grid cell distance of the cloud top or bottom is discarded, to avoid biases due to averaging over the border of the cloud.

3. COMPARISON WITH OBSERVATIONS

For the validation of the numerical work, the fly-through profiles of w and q_t are compared with [RDJ03]. The observational results are displayed in figure 2(left). The profiles are averaged over all clouds; on top of it, the rms-deviations are plotted; they are meant to give a measure of turbulence in the cloud, and do not represent the error in the mean. In figure 2(right) the corresponding LES profiles are displayed. The LES results contain flights through 5 simulations between 17.00 UTC and 21.00 UTC, approximately the flight times of the measurements, capturing clouds of 8 grid cells ($400m$). Comparing the graphs in figure 2, the corresponding graphs appear to match very well; the average numerical solution lies well within the natural variation of the observations. A difference can be noted in the amount of turbulent variation and the predicted cloud-core values of q_t, which are all slightly underestimated by the LES; it appears that LES may have a tendency to slightly enhance mixing. However the most striking features of the observations, such as the cloud edge minimum in the w-profile is clearly present and similar sized in the simulations, although the minimum in the buoyancy profile appears to be more pronounced than in the observations. Generally speaking, LES seems to be able to capture the dynamics of the cloud very well.

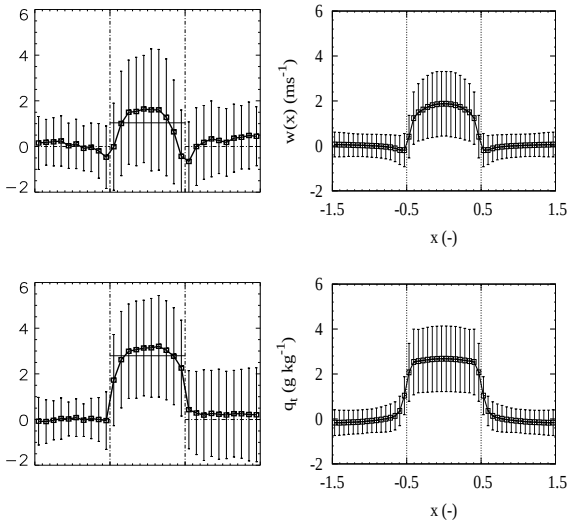

FIG. 2: Averaged in-cloud profiles of vertical velocity(top) and the total water content (bottom), of the observations by [RDJ03] (left) and of the LES (right). The cloud is centered at zero and scaled between -0.5 and 0.5. The bars denote the root mean square values of the individual measurements. These bars thus do not denote an error, but are a measure of turbulence. It can be seen that the LES results are similar to the observations.

4. INVESTIGATION OF THE VERTICAL MOMENTUM-BUDGET TERMS

In figure 2 the shell of descending air was clearly visible in both the observational data as the LES results. To investigate the origin of this shell, we can benefit from the additional information gained from the simulations, such as the individual terms of the vertical momentum equation. Neglecting the Coriolis forcing, the vertical momentum equation used in LES can be split up as follows:

$$\frac{\partial w}{\partial t} = \underbrace{-u_j \frac{\partial w}{\partial x_j}}_{A} \underbrace{+g\frac{\theta_v - \overline{\theta_v}}{\Theta_v^0}}_{B} \underbrace{-\frac{1}{\rho_0}\frac{\partial p'}{\partial z}}_{P} \underbrace{+\frac{\partial}{\partial x_j}\left[K_m\left(\frac{\partial u_j}{\partial z}+\frac{\partial w}{\partial x_j}\right)\right]}_{S} \quad (1)$$

with A the resolved advection terms, B the buoyancy force, P the vertical pressure gradient and S the parameterized unresolved subgrid diffusion (where $K_m(x,y,z)$ is the subgrid scale eddy viscosity). One or more of these forcings should be responsible for the minimum in the w-profile around the cloud edge. It can be expected that if mechanical forcing would be the main process behind the subsiding shell, the pressure gradient should be negative on the edge of the cloud. Evaporative cooling by horizontal mixing over the cloud edge, on the other hand, would result in a negative buoyancy forcing in the shell. These four terms are plotted in figure 3. From these fig-

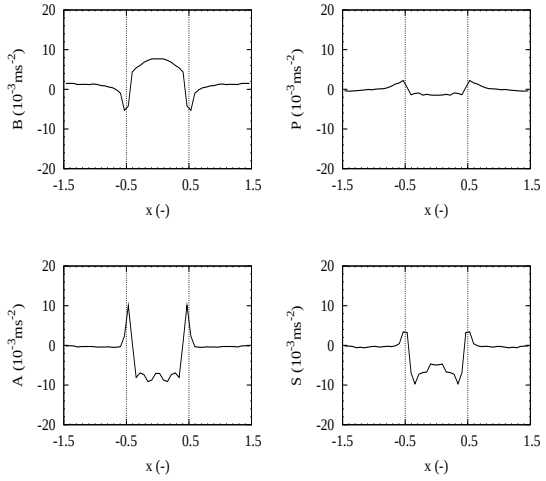

FIG. 3: Lateral profiles of the individual budget terms of the vertical momentum equation, from left to right and top to bottom: buoyancy, vertical pressure gradient, advection and subgrid diffusion. From these profiles it can be seen that the descending shell of air around the cloud is driven by evaporative cooling due to lateral mixing, since buoyancy is the only negative force at cloud edge. Moreover, the existence of the shell is counteracted by the pressure gradient force, instead of induced, which would have been the case if the shell was driven by mechanical forcing. Note that adding the four terms results in a slight unbalance; this is due to the fact that averaging over wet points only does not take the entire cloud life-cycle into account.

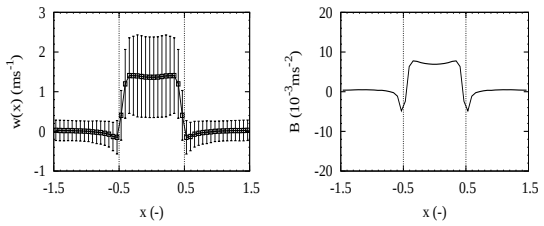

FIG. 4: As in figures 2 and 3, profiles of vertical velocity and buoyancy of the BOMEX case show a descending shell around clouds.

ures it is clear that there exists a strong minimum in buoyancy just around the cloud, whereas the pressure gradient is (like advection and subgrid diffusion) found to be counteracting the downward velocity. This indicates that the descending shell is due to evaporative cooling following lateral mixing. To investigate whether the descending shell is a specific feature of the SCMS case, or rather a more generic feature of shallow cumulus clouds, additionally the BOMEX case of marine shallow cumulus clouds is analyzed in the same way as was done for SCMS. Since BOMEX is a steady-state marine case, a much larger time window could be taken. 10 simulations of 12 hours each have been done, of which the first three hours were disregarded as spin-up. Using a height of measurement of $1000m$, 999 flights through clouds of $400m$ have been collected; the results for the vertical velocity and the buoyancy are shown in figure 4. The shapes of the profiles in figure 4 are similar to the SCMS results, including the descending shell. This suggests that the descending shell due to evaporative cooling by cloud edge mixing is a generic feature of shallow cumulus clouds.

5. MASSFLUX THROUGH THE SHELL

Looking at the relatively modest size of the dip in the $w-$profile in figure 4, one may wonder what the importance of the subsiding shell is on the interaction between the cloud and its environment. However, it has to be kept in mind that these 'fly-through' profiles are one-dimensional representations. The significance of that becomes clear when plotting the vertical mass-flux M for $400m$ sized clouds (fig. 5). On the assumption of a circular-shaped cloud, M would be:

$$M(r)dx = \rho w(r) 2\pi r dr \tag{2}$$

The contribution to M of the (slow moving) air further away from cloud-center cannot be neglected compared to the fast moving cloud-core, because of the significant area of the outer region. Looking at figure 5, 10% (black area) of the air flowing upwards through the cloud comes down directly through the shell (where $B < 0$), while another 13% (dark grey area) is dragged along downwards with the shell, in total balancing almost a quarter of the in-cloud up-flow. Looking at a crosssection of a cloud in figure 6, the shell appears to exist over the entire height

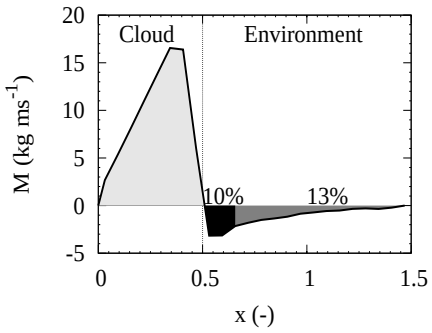

FIG. 5: The vertical massflux M through $400m$ sized clouds as a function of the distance to cloud center r for BOMEX at $1000m$ height. For small r, M goes to zero due to small size of the area. The black colored area signifies the massflux through the descending shell(around 10% of the total cloud massflux). The dark grey area is dragged downwards induced by the shell, resulting in a total of 25% of the in-cloud up-flow.

of the cloud. This ensures that since the environment has no direct interaction with the warm cloud core, it 'feels' the cloud as a negatively buoyant, downwards moving entity. The significant amount of air dragged downwards might also explain the results of [J90], where an analysis with help of Paluch diagrams suggested the presence of air of higher level origins.

6. THREE-LAYER MODEL

To gain better understanding of the role and behavior of the shell, a simple analytical model of the clouds is developed. This is done by dividing the clouds and environment into 3 sections: The environment, the cloud core, and the subsiding shell in between, each with their respective distance to cloud center, velocity and virtual potential temperature. (see figure 8). This approach is similar to ((Asai and Kashara, 1967)), who based their analysis of a shallow cumulus cloud on a two-layer model. It should be noted that it is not the aim of this analysis to develop a highly realistic model of the cloud and its surroundings, but merely to demonstrate the role evaporative cooling can play in lateral mixing. To obtain this, the assumption is made that the cloud is in steady state and that vertical gradients are negligible. Writing equation 1 down in cylindrical coordinates and applying these assumptions, it reads:

$$\frac{\partial w}{\partial t} = -\frac{1}{r}\frac{\partial}{\partial r}(ruw) + \frac{g}{\Theta_{v0}}(\theta_v - \theta_{v0}) = 0 \qquad (3)$$

The continuity equation can be integrated over the area A_n of each shell, resulting in:

$$\int_0^{2\pi}\int_{r_{n-1}}^{r_n}\left\{\frac{1}{r}\frac{\partial}{\partial r}(ru_n) + \frac{\partial w_n}{\partial z}\right\} dr d\varphi = 0 \qquad (4)$$

$$2\pi r_n u_n - 2\pi r_{n-1}u_{n-1} = 0 \qquad (5)$$

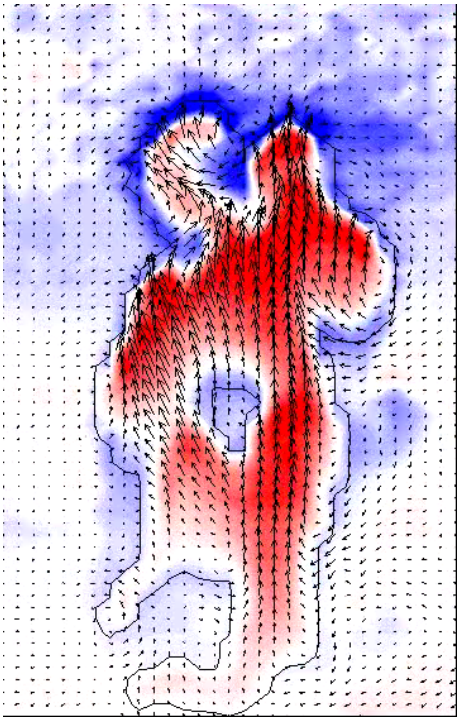

FIG. 6: A crosssection through the center of mass of a cloud. The subsiding shell is clearly visible, especially in the negative buoyancy at cloud edge.

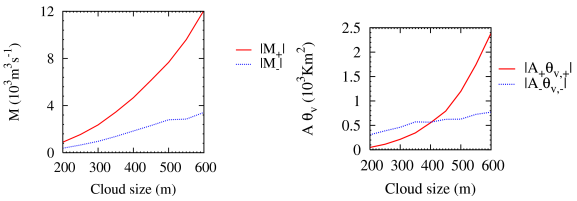

FIG. 7: The absolute values of the massflux (left) and the buoyancy flux through the cloud core (red line) and the shell (blue dotted line). For small clouds, the shell is clearly more important than for large clouds.

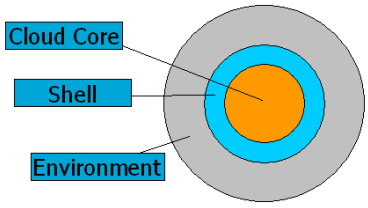

FIG. 8: The proposed model divides the cloud layer in three shells: Inside the cloud core, with positive vertical velocity and buoyancy, wrapped around it the subsiding shell with negative vertical velocity and buoyancy and finally an environmental region balancing the other two.

With $r_0 = 0$ this gives $u_n = 0$ for all $n > 0$. Integrating equation 3 over shell n now yields:

$$2\pi r_n \widetilde{uw}^n - 2\pi r_{n-1} \widetilde{uw}^{n-1} = A_n \frac{g}{\Theta_{v0}} (\Delta\theta_{vn}) \tag{6}$$

With $\Delta\theta_{vn} = \theta_{vn} - \theta_{v0}$. Since $u_n = 0$, only the fluctuations of $\widetilde{uw}^n$ are nonzero. Furthermore, normalizing the area with the size of the cloud core:

$$\sigma_n = \frac{A_n}{A_1} \sigma_1 \tag{7}$$

finally we obtain

$$r_n \widetilde{u'w'}^n - r_{n-1} \widetilde{u'w'}^{n-1} = \frac{\sigma_n r_1^2}{2\sigma_1} \frac{g\Delta\theta_{vn}}{\Theta_{v0}} \tag{8}$$

while conservation laws dictates:

$$\begin{aligned} \sum \sigma_n &= 1 \\ \sum \sigma_n \Delta\theta_{vn} &= 0 \\ \sum \sigma_n w_n &= 0 \end{aligned} \tag{9}$$

For the turbulent diffusion term $\widetilde{u'w'}^n$ closure is needed; here Prandtl mixing length theory is applied:

$$\widetilde{u'w'}^n = -K_n \left. \frac{dw}{dr} \right|_{r=r_n} = -K_n \frac{w_{n+1} - w_n}{\frac{1}{2}(r_{n+1} - r_{n-1})} \tag{10}$$

with for K_n:

$$K_n = \ell^2 \left| \frac{w_{n+1} - w_n}{\frac{1}{2}(r_{n+1} - r_{n-1})} \right| \tag{11}$$

Now only the mixing length ℓ is unknown. It seems reasonable to assume that the width of the shell is the significant lengthscale here, which yields:

$$\ell = \alpha\zeta r_1 \tag{12}$$

with von Karman constant $\alpha = 0.4$ and $\zeta = \frac{r_2 - r_1}{r_1}$ the relative width of the shell. Using the conservation laws (eq. 9 to eliminate σ_3, w_3 and $\Delta\theta_{v3}$and substituting ζ we get the following equations:

$$\frac{g\Delta\theta_{v1}}{8\alpha^2\Theta_{v0}} = \frac{\zeta^2}{(1+\zeta)^2 r_1} (w_1 - w_2)^2 \tag{13}$$

$$\frac{g\Delta\theta_{v2}}{8\alpha^2\Theta_{v0}} = -\frac{\zeta^3(2+\zeta)}{(1+\zeta)^2 r_1} (w_1 - w_2)^2 - \frac{\zeta^3(2+\zeta)}{(\sigma_1^{-0.5} - 1)^2 r_1} \left[\frac{\sigma_1 w_1 + (1-\sigma_1) w_2}{1 - \sigma_1(1+\zeta^2)} \right]^2 \tag{14}$$

where is used that $w_1 > w_3 > w_2$. Note that σ_1 denotes the cloudfraction, which is typically around 0.05 for BOMEX. To close the system assumptions have to be made regarding the in-cloud conditions. Since the shell can be regarded as a border effect, As a rough estimate the size is kept constant. Furthermore, an undiluted core is assumed, so that the buoyancy difference can be seen as the buoyancy difference between cloudbase and a level of observation. With the in cloud velocity estimated using a free fall assumption, the results are represented in figure 9. The model seems to fit the computational data quite well.

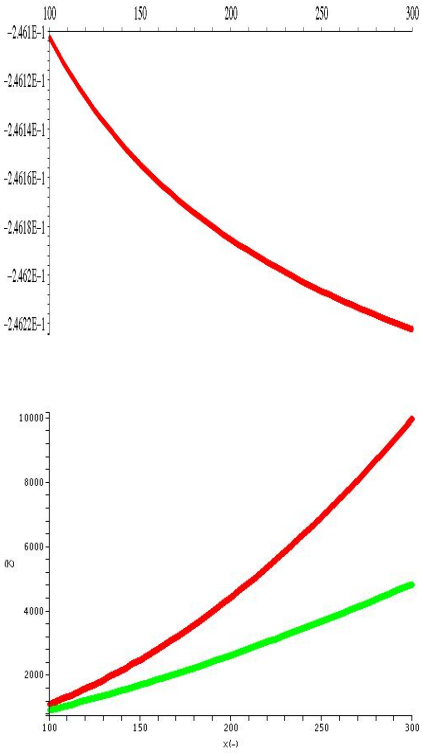

FIG. 9: The minimum virtual potential temperature (top) and the massflux (bottom) through the cloud (red line) and the shell (green line) as a function of cloudradius, as determined from the three layer model.

7. ACKNOWLEDGMENTS

The investigations were supported by the Netherlands Organization for Scientific Research (NWO). This work was sponsored by the National Computing Facilities Foundation (NCF) for the use of supercomputer facilities.

REFERENCES

Asai, T. and A. Kashara, 1967: A theoretical study of compensating downward motions associated with cumulus clouds. *Journal of the Atmospheric Sciences*, **24**(5), 487–496.

Blyth, A. M., 1993: Entrainment in cumulus clouds. *Journal of Applied Meteorology*, **32**, 626–641.

Cuijpers, J. and P. Duynkerke, 1993: Large-eddy simulation of trade wind cumulus clouds. *Journal of the Atmospheric Sciences*, **50**, 3894–3908.

Jonas, P., 1990: Observations of cumulus cloud entrainment. *Atmospheric Research*, **25**, 105–127.

Neggers, R., P. Duynkerke, and S. Rodts, 2003: Shallow cumulus convection: A validation of large-eddy simulation against aircraft and landsat observations. *Quarterly Journal of the Royal Meteorological Society*, **129**(593), 2671–2696.

Paluch, I., 1979: The entrainment mechanism in colorado cumuli. *Journal of the Atmospheric Sciences*, **36**, 2467.

Rodts, S., P. Duynkerke, and H. Jonker, 2003: Size distributions and dynamical properties of shallow cumulus clouds from aircraft observations and satellite data. *Journal of the Atmospheric Sciences*, **60**(16), 1895–1912.

Siebesma, A. and J. Cuijpers, 1995: Evaluation of parametric assumptions for shallow cumulus convection. *Journal of the Atmospheric Sciences*, **52**(6), 650–666.

Siebesma, A. P., C. S. Bretherton, A. Brown, A. Chlond, J. Cuxart, P. G. Duynkerke, H. L. Jiang, M. Khairoutdinov, D. Lewellen, C. H. Moeng, E. Sanchez, B. Stevens, and D. E. Stevens, 2003: A large eddy simulation intercomparison study of shallow cumulus convection. *Journal of the Atmospheric Sciences*, **60**(10), 1201–1219.

Stevens, B., A. S. Ackerman, B. A. Albrecht, A. R. Brown, A. Chlond, J. Cuxart, P. G. Duynkerke, D. C. Lewellen, M. K. Macvean, R. A. J. Neggers, E. Sanchez, A. P. Siebesma, and D. E. Stevens, 2001: Simulations of trade wind cumuli under a strong inversion. *Journal of the Atmospheric Sciences*, **58**(14), 1870–1891.